

Higher-resolution tropopause folding accounts for more stratospheric ozone intrusions

Samuel Bartusek^{1,2}, Yutian Wu¹, Mingfang Ting^{1,2}, Cheng Zheng¹, Arlene Fiore³, Michael Sprenger⁴, Johannes Flemming⁵

¹Lamont-Doherty Earth Observatory, Columbia University, Palisades, NY, USA

²Department of Earth and Environmental Sciences, Columbia University, New York, NY, USA

³Department of Earth, Atmospheric, and Planetary Sciences, Massachusetts Institute of Technology, Cambridge, MA, USA

⁴Institute for Atmosphere and Climate Science, ETH Zürich, Zürich, Switzerland

⁵European Centre for Medium-Range Weather Forecasts (ECMWF), Reading, UK

Key Points:

- Tropopause folding is significantly more frequent with increasing atmospheric grid-cell resolution.
- Nearly 90% of folding in ERA5 (nearly 100% of Deep folding) is unrepresented at the resolution of ERA-Interim.
- High-resolution folding is more strongly correlated with tropospheric ozone, driven by deeper and more filamentary folding.

Corresponding author: Samuel Bartusek, samuel.bartusek@columbia.edu

Abstract

Ozone in the troposphere is a pollutant and greenhouse gas, and it is crucial to better understand its transport from the ozone-rich stratosphere. Tropopause folding, wherein stratospheric air intrudes downward into the troposphere, enables stratosphere-to-troposphere ozone transport (STT). However, systematic analysis of the relationship between folding and tropospheric ozone, using data that can both capture folding’s spatial scales and accurately represent tropospheric chemistry, is lacking. Here, we compare folding in both high-resolution (0.25°) reanalysis ERA5 and low-resolution (0.75°) chemical reanalysis CAMSRA over one year. High-resolution folding is dramatically more frequent and significantly better-correlated with tropospheric ozone. In particular, folding of deep tropospheric extent is nearly 100% missing at low resolution, and folding–ozone correlations increase most with resolution along midlatitude storm tracks, where deep folding is most common. Our results imply that STT is more attributable to tropopause folding than implied by low-resolution analysis, likely associated with resolving filamentary, deep folding.

Plain Language Summary

“Tropopause folding” refers to high-altitude atmospheric events wherein the “tropopause” (the boundary separating the troposphere, the lowest atmospheric layer, from the stratosphere above it) is perturbed, “folding” downward and allowing stratospheric air to intrude into the troposphere. These intrusions can enable stratosphere-to-troposphere transport (STT) of ozone, a pollutant and greenhouse gas in the troposphere—however, how strongly such events affect tropospheric ozone remains unclear. Here, we identify tropopause folding occurrences in both high- and low-resolution representations of atmospheric motion throughout one year, and assess how strongly each representation of folding is related to the estimated movement of tropospheric ozone. First, a high-resolution view reveals that folding events are much more frequent and widespread—and penetrate further into the troposphere, becoming more filamented—than visible at lower resolution. Moreover, folding at higher resolution is more closely correlated with tropospheric ozone behavior. These findings imply that folding may exert influence over a larger proportion of ozone STT (and potentially of the overall behavior of tropospheric ozone) than is suggested by coarse representations of folding. Furthermore, they underscore the importance

of representing such skinny, filamentary features in estimates of atmospheric motion and transport of gases.

1 Introduction

Ozone in the stratosphere is beneficial to life on earth, but in the troposphere (where it is much rarer) it is a pollutant hazardous to human health and crops (Krzyzanowski & Cohen, 2008; Monks et al., 2015) and an effective greenhouse gas (Myhre et al., 2013). Understanding the sources of tropospheric ozone is thus societally and climatically important. While photochemical production is the largest source of tropospheric ozone, stratosphere-to-troposphere transport (STT) is a significant contributor (Neu et al., 2014; Hess et al., 2015; Williams et al., 2019), and stratospheric influence on tropospheric ozone is projected to strengthen due both to global-warming-related changes in the stratospheric circulation and to stratospheric ozone recovery (Hegglin & Shepherd, 2009; Hess et al., 2015; Banerjee et al., 2016; Meul et al., 2018; Akritidis et al., 2019; Fu & Tian, 2019).

The dominant mechanism for STT of air is tropopause folding (Stohl et al., 2003), wherein an intrusion of the stratosphere into the troposphere allows exchange between the two layers, increasing local upper- and mid-tropospheric ozone concentrations (Danielsen, 1968; Shapiro, 1980). Folding is responsible for large stratospheric influence on surface ozone and air-quality-exceedance events in some regions—notably the summertime eastern Mediterranean, Middle East, and Afghanistan (Tyrlis et al., 2014; Zanis et al., 2014; Akritidis et al., 2016) and the wintertime and springtime western United States (Langford et al., 1996; Langford & Reid, 1998; Langford et al., 2009; Lefohn et al., 2012; Lin et al., 2012; Skerlak et al., 2014; Lin et al., 2015; Wang et al., 2020) and Tibetan Plateau (Sprenger et al., 2003; X. L. Chen et al., 2011; X. Chen et al., 2013; Skerlak et al., 2014). However, this influence is not well constrained, and it is important to more systematically understand tropopause folding’s role in influencing ozone STT and tropospheric ozone (Beekmann et al., 1997; Skerlak et al., 2014).

Gaps in understanding the relationships between tropopause folding, ozone STT, and tropospheric ozone have persisted for decades, limited by both meteorological and chemical data. While global-scale studies have analyzed folding itself (Skerlak et al., 2015; Akritidis et al., 2021) and its role in STT (Sprenger et al., 2003; Akritidis et al., 2019), to date such analysis has been restricted to low horizontal resolution (>80 km, e.g., ERA-

Interim). However, because folding is a meso- to synoptic-scale process, capturing fold morphology and fold-related turbulent STT processes requires resolutions <50 km (Knowland et al., 2017; Buker et al., 2005; Spreitzer et al., 2019). Consequently, the frequency of “double-tropopause” structures (of which folding is one type) is significantly higher in high-resolution ERA5 versus ERA-Interim (Hoffmann & Spang, 2022). High-resolution observational evidence, although sparse and localized, has suggested that atmospheric transport structures are horizontally and vertically filamentary, characterized by thin, diffusion-resistant layers (Danielsen, 1959; Appenzeller & Davies, 1992; Appenzeller et al., 1996; Newell et al., 1996, 1999; Trickl et al., 2010, 2020). Resolution may therefore greatly impact the representation of tropopause folding and its associated transport. Second, the fidelity of reanalysis ozone (particularly tropospheric) is constrained by both observational sparseness and, crucially, a lack of integrated chemical transport models (Dragani, 2010; Knowland et al., 2017; Wargan et al., 2017; Park et al., 2020). Therefore, despite reanalysis- and observation-based research on folding and its STT and ozone impacts (largely separately), a systematic global-scale relation of tropospheric ozone to tropopause folding has remained elusive.

Characterization of tropopause folding and its relationship with tropospheric ozone therefore lacks both (1) analysis of folding in a global dataset of sufficient meteorological fidelity, and (2) analysis of its ozone impacts in a global dataset of sufficient chemical fidelity. Here, addressing both gaps, we identify folding throughout one year in both high-resolution reanalysis ERA5 and a lower-resolution chemical reanalysis CAMSRA (with meteorology assimilated nearly-identically to ERA5 but at the resolution of ERA-Interim), and assess the relationship between both folding datasets and tropospheric ozone (derived from CAMSRA). Specifically, we address the following questions:

1. How are frequencies and global distributions of folding affected by spatial resolution?
2. How is the relationship between folding and tropospheric ozone affected by folding resolution?
3. How may folding frequency or morphology differences account for differing folding–ozone relationships?
4. What do our findings imply about ozone STT associated with folding, and tropospheric transport structures generally?

2 Data and Methods

We analyze data throughout 2012 from reanalyses CAMSRA (Copernicus Atmosphere Monitoring Service Reanalysis; European Center for Medium-range Weather Forecasting [ECMWF]) and ERA5 (ECMWF Reanalysis v5). CAMSRA (Inness et al., 2019) is a new chemical reanalysis at T255 spectral horizontal resolution (0.75° , 79 km grid) and 60 vertical levels to 0.1 hPa. ERA5 (Hersbach et al., 2020) is the latest ECMWF meteorological reanalysis at T639 resolution (0.25° , 31 km) and 137 levels to 0.01 hPa. Both reanalyses are produced by ECMWF’s Integrated Forecasting System (IFS) using 4D-Var data assimilation; ERA5 uses IFS Cycle 41r2 and CAMSRA uses Cycle 42r1 (both implemented in 2016). CAMSRA meteorological fields are at the resolution of ERA-Interim (Dee et al., 2011) but produced with an updated model cycle nearly equivalent to that of ERA5 (ERA-Interim used Cycle 31r2, implemented in 2006)—therefore, the difference between CAMSRA and ERA5 meteorology is likely almost entirely due to resolution, even more strictly than between ERA-Interim and ERA5. From each reanalysis, we obtained six-hourly zonal and meridional wind components, potential temperature, and specific humidity at model levels up to 50 hPa, and surface pressure.

From CAMSRA, we also obtained ozone at pressure levels 250 hPa, 500 hPa, and 850 hPa, and a stratospheric ozone tracer (O_3S) interpolated to the same pressure levels from model levels. Unlike other reanalyses that assimilate ozone observations (such as NASA’s Modern-Era Retrospective Analysis for Research and Applications 2 [MERRA-2], and ERA5), CAMSRA employs a chemical transport model (CTM) integrated into IFS—the Carbon Bond 2005 (CB05) chemistry mechanism, derived from Transport Model 5 (Huijnen et al., 2010; Flemming et al., 2015). While two previous chemistry reanalyses from ECMWF (MACC and GEMS) also employed a CTM, it remained two-way coupled to IFS instead of directly integrated (on-line) within it, and while one other reanalysis employs a CTM (Tropospheric Chemical Reanalysis 2 [TCR-2] from the Japan Agency for Marine-Earth Science and Technology [JAMSTEC]) it is of much coarser resolution (1.1° , 27 levels). A regional study found the inclusion of a dedicated CTM in reanalyses, as opposed to a one-way meteorology-chemistry relationship, to be more determinative of tropospheric composition fidelity than other factors such as resolution (Park et al., 2020). Furthermore, CAMSRA ozone has been shown to be broadly consistent with observations in the upper troposphere during stratospheric intrusions over Europe, despite overestimation in some sites (Akritidis et al., 2022). Stratospheric ozone in CAM-

SRA is parameterized using the Cariolle scheme (Cariolle & Déqué, 1986; Cariolle & Teyssède, 2007), and subject to data assimilation. O_3S is identical to total ozone in the stratosphere, but once across the tropopause (a spatially-varying pressure threshold fixed in time) it is freely transported and subject to chemical loss and deposition, but not production. It therefore roughly represents the portion of tropospheric ozone deriving from the stratosphere, likely tending towards an upper limit.

To identify tropopause folding in CAMSRA and ERA5, we apply a modified version of the algorithm of Skerlak et al. (2015) (building on Sprenger et al., 2003; Skerlak et al., 2014). The algorithm first defines the dynamical tropopause as the lower of the ± 2 Potential Vorticity Unit (PVU) or 380 K potential temperature surface. At each timestep, folding is identified in each atmospheric column in which the tropopause is crossed in the vertical three or more times. Pressure values of the three crossings (interpolated between model levels based on the PV profile) are saved: $pmin$ and $pmax$ are the pressures of the upper and lower crossings and dp is the pressure difference between the upper and middle crossings (Figure 1a). Folded columns are classified into three depth ranges: Shallow ($50 \text{ hPa} \leq dp < 200 \text{ hPa}$), Medium ($200 \text{ hPa} \leq dp < 350 \text{ hPa}$), and Deep ($dp \geq 350 \text{ hPa}$), ignoring folding $< 50 \text{ hPa}$. However, high-PV anomalies can arise in the troposphere independently from folding (e.g., fully cut-off from the stratosphere, or generated by diabatic or surface frictional processes). Therefore, to avoid spuriously identifying folding, the algorithm labels each 3D grid cell as either troposphere, stratosphere, troposphere but high-PV, or stratosphere but low-PV. In our analysis, ERA5’s high resolution necessitated modifications to the algorithm to avoid occasional classifications of the entire stratosphere as high-PV surface-connected (therefore tropospheric) air (see details in Supplementary Information). Comparing folding identification with versus without our modifications shows them to be generally conservative, reducing folding frequency (Figure S1).

Analysis year 2012 was chosen in order to minimize discontinuities in assimilated ozone data and provide the most recent data free of known instrumentation biases (affecting CAMSRA ozone from 2013 onwards; Inness et al., 2019; Wagner et al., 2021). Folding frequencies in 2012 are roughly consistent with the 1979–2014 average (from ERA-Interim; Figure S1). Because a single year was used, ozone and folding fields were deseasonalized by removing smoothed local monthly averages before correlation analysis.

3 Results

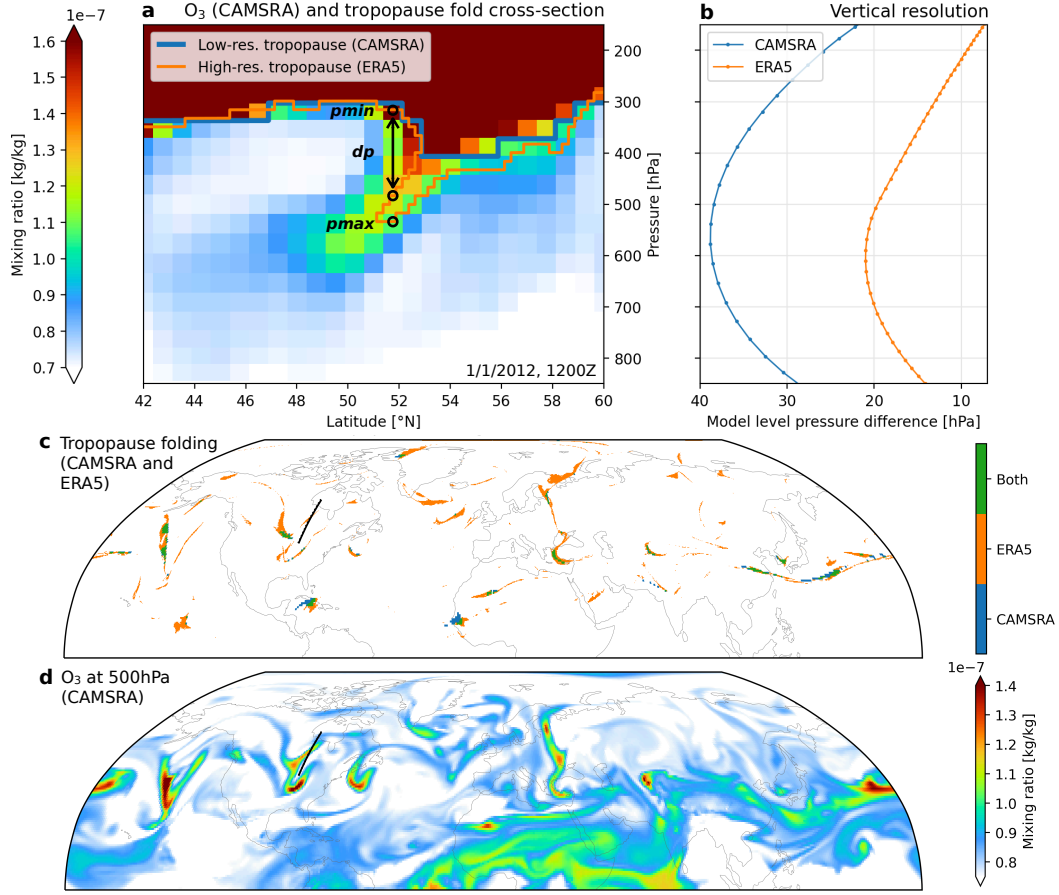


Figure 1. Comparison of a tropopause fold cross-section, vertical resolution, and snapshot folding and mid-tropospheric ozone in CAMSRA and ERA5. *a*): Dynamical tropopauses in CAMSRA and ERA5, and ozone from CAMSRA, along a latitudinal cross-section (line in *c–d*) on 1/1/2012 (1200Z). The ERA5 tropopause is folded throughout a range of columns ($\sim 51^{\circ}$ – $53^{\circ}N$); pressure parameters $pmin$, dp , and $pmax$ produced by the folding identification algorithm (see Data and Methods) are illustrated for one column. *b*): CAMSRA and ERA5 vertical resolution; dots indicate model levels. *c–d*): All columns with folding identified in CAMSRA, ERA5, or both (*c*), and 500 hPa ozone (*d*), during the example timestep.

We first show an example of tropopause folding captured only at higher resolution: a latitudinal cross-section displays a fold in the ERA5 tropopause that CAMSRA’s tropopause is too coarse to resolve (Figure 1a). Meanwhile, in this fold’s vicinity, ozone (in CAMSRA) intrudes from the stratosphere into the troposphere—hence, while the intrusion

itself is resolved by CAMSRA, its relationship to folding is only captured by a higher-
 resolution tropopause. More broadly, during the example timestep, folding is much more
 widespread in ERA5, and reveals stronger correspondence with mid-tropospheric ozone,
 overlapping with many filamentary ozone structures that CAMSRA folding does not (Fig-
 ure 1c–d). This improved correspondence generally persists across the 250, 500, and 850
 hPa levels for both total (O_3) and stratosphere-sourced (O_3S) ozone, although the gen-
 eral folding–ozone relationship weakens in the tropics and at 850 hPa (Figure S2). This
 cross-section suggests an important role for vertical resolution—accordingly, ERA5’s is
 at least roughly double CAMSRA’s throughout the troposphere (Figure 1b)—while a
 geographic perspective also emphasizes horizontal resolution (Figure 1c–d). Overall, it
 appears common that ozone intrusions are only revealed to be associated with folding
 when the tropopause is seen at high-enough resolution. In such cases, the transport it-
 self occurs at scales larger than the ERA5-identified folding—CAMSRA ozone is advected
 by resolved winds—entering the troposphere despite an unfolded (coarsely-resolved) tropopause.
 (Meanwhile, it is possible that alternative tropopause definitions may identify folding
 in better alignment with transport at lower resolution, especially if based on tracers, but
 this is beyond our scope).

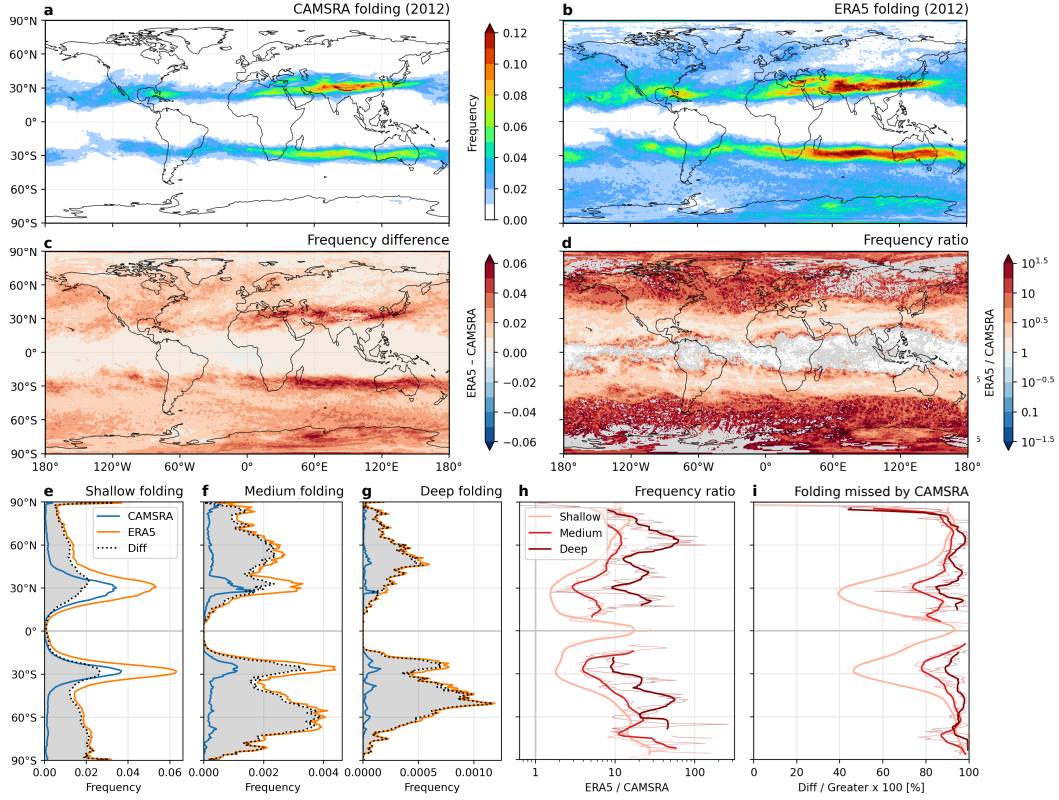


Figure 2. One-year tropopause folding frequencies in CAMSRA and ERA5. *a–b*): Folding frequency throughout 2012, in fractional units ($0.1 = 36.5$ days per year). *c–d*): Frequency difference (ERA5 – CAMSRA) and ratio (ERA5 / CAMSRA). *e–g*): Zonal-mean frequency of Shallow, Medium, and Deep folding (note x -axis scales). *h–i*): Zonal-mean frequency ratio and percentage of folding missed by the lower-frequency dataset (i.e., the frequency difference in *c*) as a percentage of the greater of the two at each grid cell) separated by depth range, with running 10° means.

Expanding our analysis to one year, we find that folding frequency increases nearly everywhere from CAMSRA to ERA5 (Figure 2a–c). Vertical resolution likely plays an important role: folds are more often below model-level resolution in CAMSRA than ERA5, with ERA5 folds largely occurring at resolved scales (Figure S3). Their frequency difference (Figure 2c) resembles the underlying distributions (largest along the subtropical jets [STJs], especially over the South Indian Ocean, Middle East, and North Africa), most closely mirroring ERA5’s. However, relative frequency differences (Figure 2d) reveal where CAMSRA particularly under-represents folding, highlighting areas with generally rarer folding. Over much of the extratropics, folding increases >10 -fold between

208 datasets; many areas with zero CAMSRA folding approach 2% in ERA5. Additionally,
 209 while absolute frequency increases are largest for shallower folds (due to their greater
 210 prevalence), relative increases are strongest for deeper folds (Figure 2e–i). Furthermore,
 211 zonal-mean distributions of Medium and Deep folding in CAMSRA fail to capture to first
 212 order their prominent midlatitude peaks evident in ERA5. Zonal-mean frequency ratio
 213 (Figure 2h) and percentage of ERA5 folding missed by CAMSRA (Figure 2i) confirm
 214 that deeper folding is more likely to be uncaptured at low resolution. Specifically, while
 215 around half of ERA5 folding is missed by CAMSRA at its dominant latitudes (rising to
 216 >90% in the extratropics and overall nearly 90% on average), nearly 100% of Deep fold-
 217 ing is missed almost everywhere (Figure 2i, S4).

218 The finding that lower resolution disproportionately misses deeper folding likely
 219 reflects that as intrusions extend deeper into the troposphere they tend to become more
 220 filamentary, hence more difficult to resolve vertically. Accordingly, the distribution of av-
 221 erage folding depth (Figure S5) very strongly predicts that of frequency ratio (Figure
 222 2d). Such an underestimation of specifically deeper intrusions into the troposphere may
 223 be consequential towards capturing folding’s relationship with tropospheric ozone: there-
 224 fore, we next investigate the influence of folding resolution on temporal correlations be-
 225 tween folding activity and ozone STT.

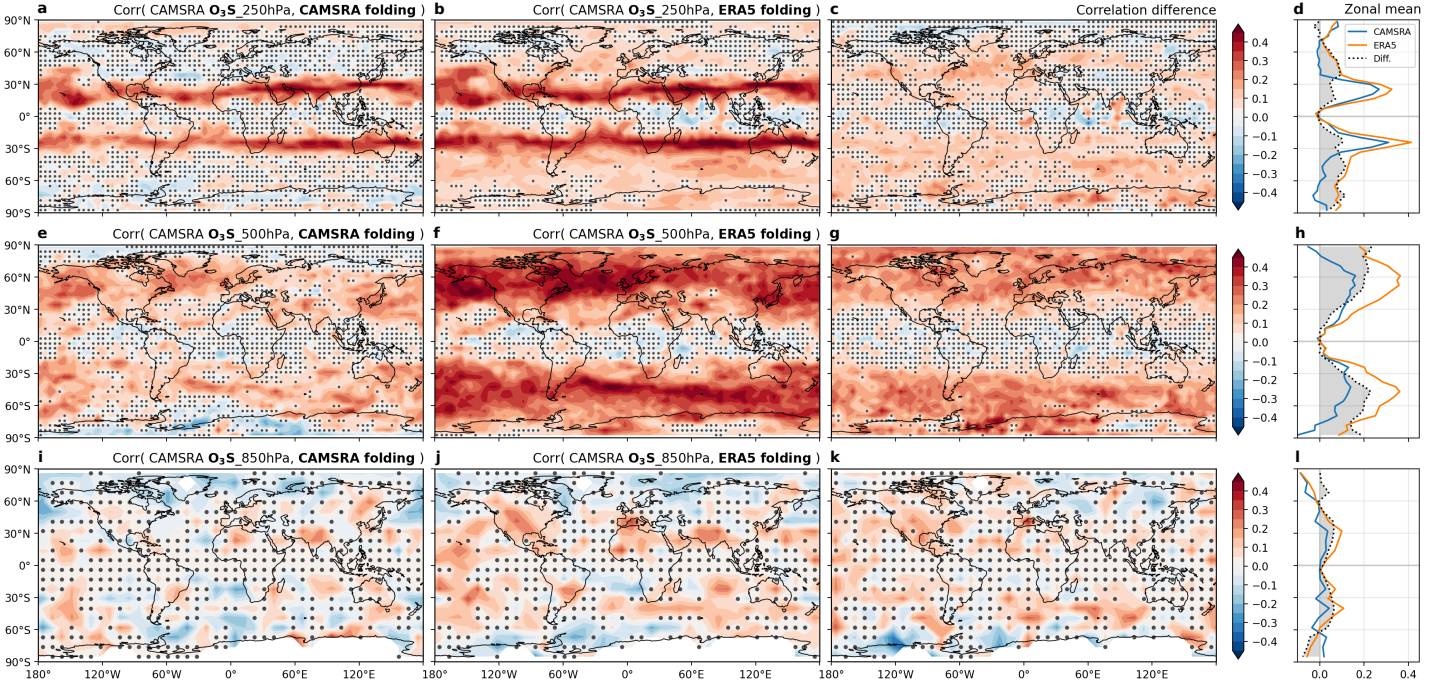


Figure 3. Correlations between tropopause folding and CAMSRA ozone at three pressure levels. *a*): Spearman’s rank correlation between folding occurrence in CAMSRA and stratospheric ozone tracer (O_3S , from CAMSRA) at 250 hPa, throughout 2012, dotted where insignificant ($\alpha = 0.05$). ***b*):** As in *a*) but for ERA5 folding. In other words, between *a*) and *b*) the same O_3S field is correlated against two different folding fields. ***c*):** Difference in correlation coefficients, dotted where insignificant. ***d*):** Zonal means of *a*–*c*). ***e*–*l*):** As in *a*–*d*) but for O_3S at 500 and 850 hPa. Fields are coarsened to $4.5^\circ \times 4.5^\circ$ (250, 500 hPa) or $9^\circ \times 9^\circ$ (850 hPa), and smoothed by one-day (500 hPa) or three-day (850 hPa) running means, to better capture non-local ozone impacts of folding; only Medium and Deep folding is considered at 850 hPa.

Accompanying increased fold frequency with increased resolution, the correlation between folding and tropospheric O_3S (to most directly reflect STT) significantly strengthens, outside the tropics (Figure 3). The relationship between folding and 250 hPa O_3S closely follows underlying fold frequency distributions (Figure 2a–b, e): correlation maximizes along STJs, reaching 0.40 for CAMSRA and 0.45 for ERA5, and generally strengthens with higher folding frequency (Figure 3a–d). However, correlations strengthen most where relative (Figure 2d) rather than absolute (Figure 2c) frequency differences are highest, increasing by ~ 0.2 from near-zero in CAMSRA throughout much of the extratropics (where 250 hPa most represents the upper troposphere / lower stratosphere region).

At 500 hPa, O_3S is most correlated to folding in the extratropics, emphasizing storm tracks rather than STJs (Figure 3e–f, h). Correlations strongly mirror folding depth (Figure S5), implying that deeper midlatitude folds, though rarer than STJ-related folds, are more powerfully associated with mid-tropospheric ozone. O_3S at 500 hPa is roughly twice as correlated to ERA5 folding as to CAMSRA folding, reaching ~ 0.4 over widespread regions, and correlation improvements again reflect relative frequency increases, as well as Medium and Deep folding differences (Figure S6). At 850 hPa, O_3S is much less correlated with folding overall (Figure 3i–j, l), perhaps partially reflecting that folding-related ozone impacts may be spatially offset from folding itself after transport into the lower troposphere. However, O_3S correlation with ERA5 folding reveals maxima in known hotspots of strong stratospheric and folding influence on near-surface ozone (not well captured by CAMSRA folding), including western North America, the Tibetan Plateau, the Mediterranean, and storm track regions (Skerlak et al., 2014). Increases in correlation generally follow Medium and Deep fold frequency increases—strongest over North America and the eastern Pacific and Southern Ocean storm tracks (Figure 3k).

Since O_3S 's stronger relation to ERA5 than CAMSRA folding occurs alongside *more frequent* folding, we argue that ozone STT may be more attributable to folding than low-resolution folding implies. In other words, ozone STT occurring without folding in CAMSRA is revealed to occur in the vicinity of folding at smaller scales, as suggested by Figure 1. Altogether, correlations strengthen most at the approximate latitudes of maximum ozone STT—in midlatitudes, poleward of STJs (Hsu & Prather, 2009; Skerlak et al., 2014)—implying the relevance of these changes for overall STT. Furthermore, Figure 3's correlation results are generally consistent when substituting total ozone for O_3S , (Figure S7)—except at 850 hPa, where its drivers are very diverse—suggesting that folding-related O_3S is important to total (free-tropospheric) ozone.

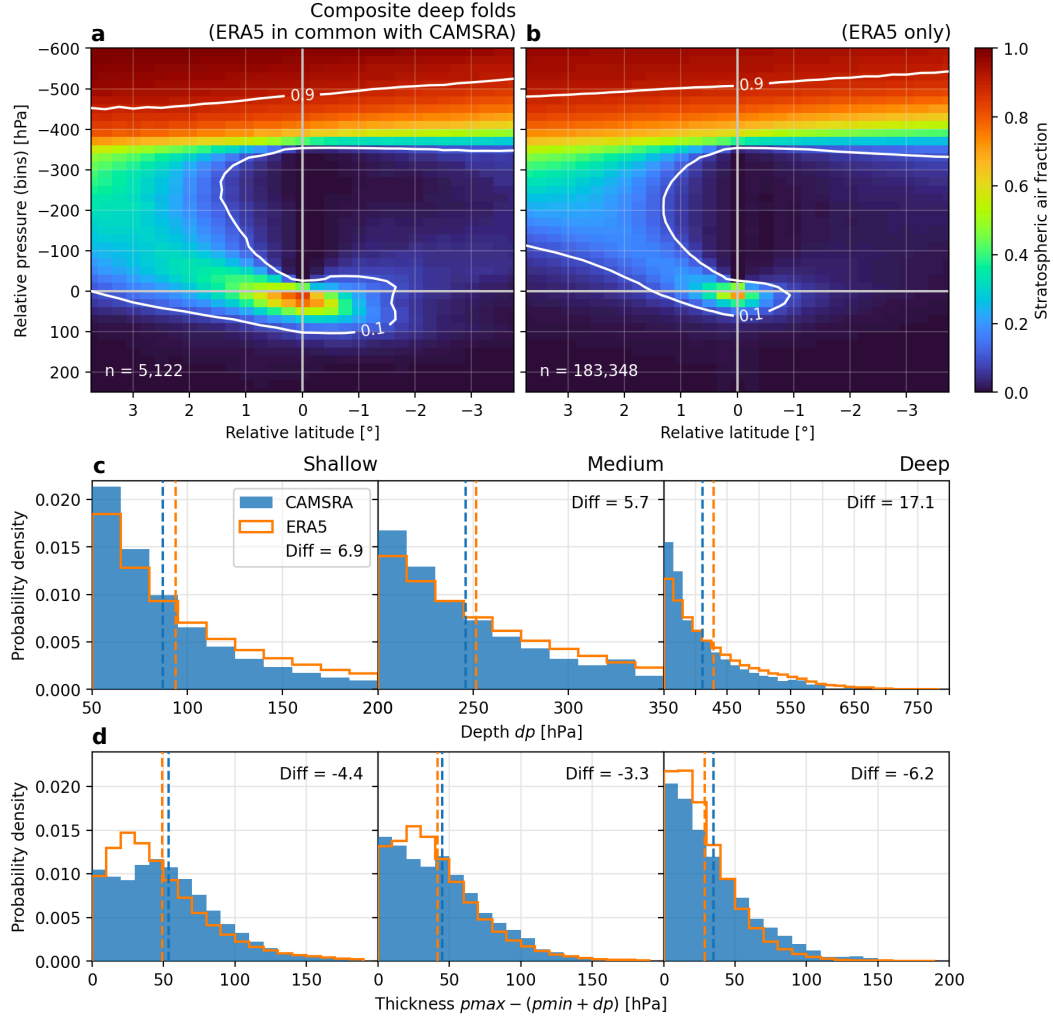


Figure 4. Tropopause folding morphology in CAMSRA and ERA5. *a–b*): Composited latitudinal cross-sections of Deep folds in ERA5 (i.e., throughout ranges of columns where folding depth dp exceeds 350 hPa, centered horizontally on the column of smallest dp and vertically on that column’s middle tropopause crossing), for folding identified in both ERA5 and CAMSRA simultaneously (*a*) versus only in ERA5 (*b*). The composited field is a binary label delineating troposphere (0) versus stratosphere (1), producing an average fold morphology; 0.1 and 0.9 contours are indicated. *c*): Histograms of dp for folding in CAMSRA and ERA5 in each depth category, with means compared. *d*): As in *c*) but for folding thickness (the pressure difference between the lowest and middle tropopause crossings, $p_{max} - (p_{min} + dp)$).

Following Figure 3’s suggestion of deeper folding’s role in strengthening ozone correlations, we directly investigate fold morphology, confirming that higher-resolution folding is both deeper and thinner, especially for Deep folding (Figure 4). Composites of $\sim 190,000$

Deep fold cross-sections in ERA5 compare folding captured by both CAMSRA and ERA5 with that only captured by ERA5 (Figure 4a–b). To compare fold morphology, we composite a binary label field that geometrically delineates the stratosphere and troposphere. Cross-sections are fixed around folds’ column of minimum depth (exceeding 350 hPa) and their middle tropopause crossing in that column (see Figure 4 caption), so that fold depth (negative pressures) and thickness (positive pressures) can both be compared across cross-sections. These cross-sections capture only folds’ latitudinal component; however, we note that even primarily-longitudinal folds likely still express in latitude (e.g., Figure 1’s example). From CAMSRA to ERA5, the 0.1 (90% stratospheric) contour thins everywhere along the composite fold, indicating decreased thickness—meanwhile, the 0.9 contour rises further above the fold, indicating increased depth (Figure 4a). Moreover, depth and thickness histograms (Figure 4c–d) quantitatively confirm that with increasing resolution, folding becomes deeper but thinner, consistently across folding depth categories (geospatially resolved in Figure S8). Deep folding is most affected, becoming on average 17 hPa deeper and 6 hPa thinner. Furthermore, in columns where ERA5 identifies Deep folding but CAMSRA fails, CAMSRA almost exclusively identifies no folding rather than simulating Medium or Shallow folding (Figure S9), confirming that CAMSRA specifically underresolves the tips of intrusions.

Figure 4 therefore provides evidence that resolving deeper, thinner folding is particularly responsible for uncovering stronger relationships between folding and tropospheric ozone. Specifically, with higher-resolution folding, ozone anomalies at greater distance from the tropopause may remain attributable to folding activity, as epitomized by Figure 1a’s cross-section: the fold tip in ERA5 extends deeper than in CAMSRA (which finds no fold), overlapping with more of the underlying ozone intrusion and thereby revealing that deeper parts of it are attributable to folding.

4 Conclusions and Discussion

In this study, we identified tropopause folding in two reanalyses—high-resolution ERA5 and lower-resolution chemical reanalysis CAMSRA (providing nearly identical meteorology but at the resolution of ERA-Interim). We compared the distribution and characteristics of folding in ERA5 (the highest-resolution such analysis to date) to those in CAMSRA, and assessed the relationships of folding at both resolutions with tropospheric ozone (from CAMSRA), to examine folding’s role in the behavior of tropospheric ozone and its transport from the stratosphere. Our conclusions and their implications are as follows:

1. Higher-resolution folding is markedly more frequent. Between datasets, frequency increases most along the subtropical jets and for shallower folds, but increases *relatively* most in the extratropics and for deeper folds (~ 10 – 100 -fold). Deep folding is nearly 100% unrepresented at lower resolution, as is $\sim 90\%$ of all folding.
2. Higher-resolution folding reveals significantly stronger correlations between folding and upper- and mid-tropospheric O_3S (stratospheric ozone tracer), especially where relative fold frequency increases are greatest and folds are deeper.
3. Higher-resolution folding’s correlation with near-surface O_3S highlights known hotspots of stratospheric ozone influence uncaptured by low-resolution folding.
4. Correlations of folding with O_3S and with total ozone are largely consistent with each other (above 850 hPa).
5. Increased resolution reveals folding to be deeper and thinner, suggesting that such folding may contribute significantly to folding–ozone correlations.

Together, our results suggest that ozone STT and tropospheric ozone are more systematically associated with tropopause folding than implied based on low-resolution folding. Specifically, of the ozone STT commonly occurring despite an unfolded (coarsely-resolved) tropopause in CAMSRA, much is revealed to be occurring in the vicinity of smaller-scale folding that is only visible at higher resolution. While this work compares one (low-resolution) ozone dataset against two different folding datasets, future work will also assess ozone at high resolution to understand folding-associated STT in greater detail.

While no studies have as comprehensively addressed both folding and its relationship to ozone transport, several have indicated the significance of folding in such processes: localized observational and process-based studies have demonstrated strong ozone STT within intrusions, extending deep into the troposphere, and broader-scale studies have noted the important influence of stratospheric ozone on tropospheric ozone (Langford et al., 1996; Langford & Reid, 1998; Langford et al., 2009; Lefohn et al., 2012; Hess et al., 2015; Neu et al., 2014; Skerlak et al., 2019; Williams et al., 2019; Wang et al., 2020). While folding’s importance to STT of air is well established (Stohl et al., 2003), such a systematic linkage to specifically ozone STT is lacking. Here, we provide systematic evidence that higher-resolution folding accounts for a larger proportion of ozone STT than lower-resolution folding. Our findings are specifically consistent with midlatitude-cyclone-associated folding representing a primary STT mechanism (with cyclone dry intrusions previously found to contribute 42% of NH ozone STT; Jaeglé et al., 2017). We show that, although ozone STT is known to be strongest along storm tracks (Skerlak et al., 2014; Hsu & Prather, 2009), its linkage with folding in these areas has remained uncaptured by low-resolution folding climatologies, which underrepresent midlatitude folding due to its smaller scales.

Furthermore, the particular importance of thinner and deeper folding to tropospheric ozone underscores atmospheric transport’s filamentary nature. Transport in the stable, highly-sheared free troposphere dominantly occurs in thin layers and plumes that filament, resisting diffusion (Newell et al., 1999; Stoller et al., 1999; Thouret et al., 2000; Heald et al., 2003). Consequently, high-concentration layers are known to enable strong localized stratospheric influence on near-surface (Trickl et al., 2010, 2020) and mid-tropospheric (Trickl et al., 2011) ozone. However, current global models fail to represent transport plumes’ observed persistence due to resolution-related over-diffusion (Eastham & Jacob, 2017; Zhuang et al., 2018). Our results imply that such small-scale structures are systematically representative of tropospheric ozone and STT, so that representing such filamentary processes in reanalysis and model simulations is crucial to accurately simulating tropospheric ozone and its transport.

Acknowledgments

This work was supported by NSF Award AGS-1802248 (S. B. and Y. W.) and NSF OPP-1825858 (M. T., Y. W. and C. Z.).

Open Research

Data Availability Statement

All reanalysis data is publicly available from the ECMWF at <https://cds.climate.copernicus.eu/cdsapp#!/dataset/reanalysis-era5-pressure-levels?tab=overview> (ERA5) and <https://ads.atmosphere.copernicus.eu/cdsapp#!/dataset/cams-global-reanalysis-eac4?tab=overview> (CAMSRA). Tropopause folding identification algorithm is available at [insert Zenodo DOI when uploaded]. Code to reproduce the figures and other results is available at [insert Zenodo DOI when uploaded].

References

- Akritidis, D., Pozzer, A., Flemming, J., Inness, A., Nédélec, P., & Zanis, P. (2022). A process-oriented evaluation of cams reanalysis ozone during tropopause folds over europe for the period 2003–2018. *Atmospheric Chemistry and Physics Discussions*, 1–23.
- Akritidis, D., Pozzer, A., Flemming, J., Inness, A., & Zanis, P. (2021). A global climatology of tropopause folds in cams and merra-2 reanalyses. *Journal of Geophysical Research: Atmospheres*, 126(8), e2020JD034115. doi: 10.1029/2020JD034115
- Akritidis, D., Pozzer, A., & Zanis, P. (2019, Nov). On the impact of future climate change on tropopause folds and tropospheric ozone. *Atmospheric Chemistry and Physics*, 19(22), 14387–14401. doi: <https://doi.org/10.5194/acp-19-14387-2019>
- Akritidis, D., Pozzer, A., Zanis, P., Tyrlis, E., Škerlak, B., Sprenger, M., & Lelieveld, J. (2016, Nov). On the role of tropopause folds in summertime tropospheric ozone over the eastern mediterranean and the middle east. *Atmospheric Chemistry and Physics*, 16(21), 14025–14039. doi: 10.5194/acp-16-14025-2016
- Appenzeller, C., & Davies, H. C. (1992, Aug). Structure of stratospheric intrusions into the troposphere. *Nature*, 358(63876387), 570–572. doi: 10.1038/358570a0
- Appenzeller, C., Davies, H. C., & Norton, W. A. (1996). Fragmentation of stratospheric intrusions. *Journal of Geophysical Research: Atmospheres*, 101(D1), 1435–1456. doi: 10.1029/95JD02674

- 381 Banerjee, A., Maycock, A. C., Archibald, A. T., Abraham, N. L., Telford, P.,
382 Braesicke, P., & Pyle, J. A. (2016, Mar). Drivers of changes in stratospheric
383 and tropospheric ozone between year 2000 and 2100. *Atmospheric Chemistry*
384 *and Physics*, 16(5), 2727–2746. doi: 10.5194/acp-16-2727-2016
- 385 Beekmann, M., Ancellet, G., Blonsky, S., De Muer, D., Ebel, A., Elbern, H., ...
386 Van Haver, P. (1997, Nov). Regional and global tropopause fold occurrence
387 and related ozone flux across the tropopause. *Journal of Atmospheric Chem-*
388 *istry*, 28(1), 29–44. doi: 10.1023/A:1005897314623
- 389 Buker, M. L., Hitchman, M. H., Tripoli, G. J., Pierce, R. B., Browell, E. V., & Av-
390 ery, M. A. (2005). Resolution dependence of cross-tropopause ozone transport
391 over east asia. *Journal of Geophysical Research: Atmospheres*, 110(D3).
392 Retrieved from [https://agupubs.onlinelibrary.wiley.com/doi/abs/](https://agupubs.onlinelibrary.wiley.com/doi/abs/10.1029/2004JD004739)
393 [10.1029/2004JD004739](https://doi.org/10.1029/2004JD004739) doi: <https://doi.org/10.1029/2004JD004739>
- 394 Cariolle, D., & Déqué, M. (1986). Southern hemisphere medium-scale waves
395 and total ozone disturbances in a spectral general circulation model. *Jour-*
396 *nal of Geophysical Research: Atmospheres*, 91(D10), 10825–10846. doi:
397 [10.1029/JD091iD10p10825](https://doi.org/10.1029/JD091iD10p10825)
- 398 Cariolle, D., & Teyssèdre, H. (2007, May). A revised linear ozone photochemistry
399 parameterization for use in transport and general circulation models: multi-
400 annual simulations. *Atmospheric Chemistry and Physics*, 7(9), 2183–2196. doi:
401 [10.5194/acp-7-2183-2007](https://doi.org/10.5194/acp-7-2183-2007)
- 402 Chen, X., Añel, J. A., Su, Z., Torre, L. d. l., Kelder, H., Peet, J. v., & Ma, Y. (2013,
403 Feb). The deep atmospheric boundary layer and its significance to the strato-
404 sphere and troposphere exchange over the tibetan plateau. *PLOS ONE*, 8(2),
405 e56909. doi: [10.1371/journal.pone.0056909](https://doi.org/10.1371/journal.pone.0056909)
- 406 Chen, X. L., Ma, Y. M., Kelder, H., Su, Z., & Yang, K. (2011, May). On the be-
407 haviour of the tropopause folding events over the tibetan plateau. *Atmospheric*
408 *Chemistry and Physics*, 11(10), 5113–5122. doi: [10.5194/acp-11-5113-2011](https://doi.org/10.5194/acp-11-5113-2011)
- 409 Danielsen, E. F. (1959, Jun). The laminar structure of the atmosphere and its re-
410 lation to the concept of a tropopause. *Archiv für Meteorologie, Geophysik und*
411 *Bioklimatologie, Serie A*, 11(3), 293–332. doi: [10.1007/BF02247210](https://doi.org/10.1007/BF02247210)
- 412 Danielsen, E. F. (1968, May). Stratospheric-tropospheric exchange based on radioac-
413 tivity, ozone and potential vorticity. *Journal of Atmospheric Sciences*, 25(3),

- 502–518. doi: 10.1175/1520-0469(1968)025<0502:STEBOR>2.0.CO;2
- Dee, D. P., Uppala, S. M., Simmons, A. J., Berrisford, P., Poli, P., Kobayashi, S., . . .
 others (2011). The ERA-Interim reanalysis: Configuration and performance
 of the data assimilation system. *Quarterly Journal of the royal meteorological
 society*, 137(656), 553–597.
- Dragani, R. (2010). *On the quality of the era-interim ozone reanalyses. part ii com-
 parisons with satellite data*. ECMWF.
- Eastham, S. D., & Jacob, D. J. (2017, Feb). Limits on the ability of global eulerian
 models to resolve intercontinental transport of chemical plumes. *Atmospheric
 Chemistry and Physics*, 17(4), 2543–2553. doi: 10.5194/acp-17-2543-2017
- Flemming, J., Huijnen, V., Arteta, J., Bechtold, P., Beljaars, A., Blechschmidt, A.-
 M., . . . Tsikerdekis, A. (2015, Apr). Tropospheric chemistry in the integrated
 forecasting system of ecmwf. *Geoscientific Model Development*, 8(4), 975–1003.
 doi: 10.5194/gmd-8-975-2015
- Fu, T.-M., & Tian, H. (2019, Sep). Climate change penalty to ozone air quality:
 Review of current understandings and knowledge gaps. *Current Pollution Re-
 ports*, 5(3), 159–171. doi: 10.1007/s40726-019-00115-6
- Heald, C. L., Jacob, D. J., Fiore, A. M., Emmons, L. K., Gille, J. C., Deeter, M. N.,
 . . . Fuelberg, H. E. (2003). Asian outflow and trans-pacific transport of carbon
 monoxide and ozone pollution: An integrated satellite, aircraft, and model per-
 spective. *Journal of Geophysical Research: Atmospheres*, 108(D24). Retrieved
 from <https://onlinelibrary.wiley.com/doi/abs/10.1029/2003JD003507>
 doi: 10.1029/2003JD003507
- Hegglin, M. I., & Shepherd, T. G. (2009, Oct). Large climate-induced changes in ul-
 traviolet index and stratosphere-to-troposphere ozone flux. *Nature Geoscience*,
 2(10), 687–691. doi: 10.1038/ngeo604
- Hersbach, H., Bell, B., Berrisford, P., Hirahara, S., Horányi, A., Muñoz-Sabater,
 J., . . . Thépaut, J.-N. (2020). The era5 global reanalysis. *Quarterly
 Journal of the Royal Meteorological Society*, 146(730), 1999–2049. doi:
<https://doi.org/10.1002/qj.3803>
- Hess, P., Kinnison, D., & Tang, Q. (2015, Mar). Ensemble simulations of the role
 of the stratosphere in the attribution of northern extratropical tropospheric
 ozone variability. *Atmospheric Chemistry and Physics*, 15(5), 2341–2365. doi:

- 10.5194/acp-15-2341-2015
- Hoffmann, L., & Spang, R. (2022). An assessment of tropopause characteristics of the ERA5 and ERA-Interim meteorological reanalyses. *Atmospheric Chemistry and Physics*, 22(6), 4019–4046.
- Hsu, J., & Prather, M. J. (2009). Stratospheric variability and tropospheric ozone. *Journal of Geophysical Research: Atmospheres*, 114(D6). Retrieved from <https://onlinelibrary.wiley.com/doi/abs/10.1029/2008JD010942> doi: 10.1029/2008JD010942
- Huijnen, V., Williams, J., van Weele, M., van Noije, T., Krol, M., Dentener, F., ... Pätz, H.-W. (2010, Oct). The global chemistry transport model tm5: description and evaluation of the tropospheric chemistry version 3.0. *Geoscientific Model Development*, 3(2), 445–473. doi: 10.5194/gmd-3-445-2010
- Inness, A., Ades, M., Agustí-Panareda, A., Barré, J., Benedictow, A., Blechschmidt, A.-M., ... Suttie, M. (2019, Mar). The cams reanalysis of atmospheric composition. *Atmospheric Chemistry and Physics*, 19(6), 3515–3556. doi: 10.5194/acp-19-3515-2019
- Jaeglé, L., Wood, R., & Wargan, K. (2017). Multiyear composite view of ozone enhancements and stratosphere-to-troposphere transport in dry intrusions of northern hemisphere extratropical cyclones. *Journal of Geophysical Research: Atmospheres*, 122(24), 13,436–13,457. doi: 10.1002/2017JD027656
- Knowland, K. E., Ott, L. E., Duncan, B. N., & Wargan, K. (2017). Stratospheric intrusion-influenced ozone air quality exceedances investigated in the nasa merra-2 reanalysis. *Geophysical Research Letters*, 44(20), 10,691–10,701. doi: <https://doi.org/10.1002/2017GL074532>
- Krzyzanowski, M., & Cohen, A. (2008, Jun). Update of who air quality guidelines. *Air Quality, Atmosphere & Health*, 1(1), 7–13. doi: 10.1007/s11869-008-0008-9
- Langford, A., Aikin, K., Eubank, C., & Williams, E. (2009). Stratospheric contribution to high surface ozone in Colorado during springtime. *Geophysical Research Letters*, 36(12).
- Langford, A., Masters, C., Proffitt, M., Hsie, E.-Y., & Tuck, A. (1996). Ozone measurements in a tropopause fold associated with a cut-off low system. *Geophysical research letters*, 23(18), 2501–2504.

- 480 Langford, A., & Reid, S. (1998). Dissipation and mixing of a small-scale strato-
481 spheric intrusion in the upper troposphere. *Journal of Geophysical Research:*
482 *Atmospheres*, 103(D23), 31265–31276.
- 483 Lefohn, A. S., Wernli, H., Shadwick, D., Oltmans, S. J., & Shapiro, M. (2012,
484 Dec). Quantifying the importance of stratospheric-tropospheric trans-
485 port on surface ozone concentrations at high- and low-elevation monitoring
486 sites in the united states. *Atmospheric Environment*, 62, 646–656. doi:
487 10.1016/j.atmosenv.2012.09.004
- 488 Lin, M., Fiore, A. M., Cooper, O. R., Horowitz, L. W., Langford, A. O., Levy, H.,
489 ... Senff, C. J. (2012). Springtime high surface ozone events over the west-
490 ern united states: Quantifying the role of stratospheric intrusions. *Journal*
491 *of Geophysical Research: Atmospheres*, 117(D21). Retrieved from [https://](https://agupubs.onlinelibrary.wiley.com/doi/abs/10.1029/2012JD018151)
492 agupubs.onlinelibrary.wiley.com/doi/abs/10.1029/2012JD018151 doi:
493 <https://doi.org/10.1029/2012JD018151>
- 494 Lin, M., Fiore, A. M., Horowitz, L. W., Langford, A. O., Oltmans, S. J., Tarasick,
495 D., & Rieder, H. E. (2015, May). Climate variability modulates western us
496 ozone air quality in spring via deep stratospheric intrusions. *Nature Communi-*
497 *cations*, 6(11), 7105. doi: 10.1038/ncomms8105
- 498 Meul, S., Langematz, U., Kröger, P., Oberländer-Hayn, S., & Jöckel, P. (2018,
499 Jun). Future changes in the stratosphere-to-troposphere ozone mass flux
500 and the contribution from climate change and ozone recovery. *Atmospheric*
501 *Chemistry and Physics*, 18(10), 7721–7738. doi: [https://doi.org/10.5194/](https://doi.org/10.5194/acp-18-7721-2018)
502 [acp-18-7721-2018](https://doi.org/10.5194/acp-18-7721-2018)
- 503 Monks, P. S., Archibald, A. T., Colette, A., Cooper, O., Coyle, M., Derwent,
504 R., ... Williams, M. L. (2015, Aug). Tropospheric ozone and its precur-
505 sors from the urban to the global scale from air quality to short-lived cli-
506 mate forcer. *Atmospheric Chemistry and Physics*, 15(15), 8889–8973. doi:
507 10.5194/acp-15-8889-2015
- 508 Myhre, G., Shindell, D., Bréon, F.-M., Collins, W., Fuglestad, J., Huang, J.,
509 ... Zhang, H. (2013). Anthropogenic and natural radiative forcing. In
510 T. F. Stocker et al. (Eds.), *Climate change 2013: The physical science basis.*
511 *contribution of working group i to the fifth assessment report of the intergov-*
512 *ernmental panel on climate change* (pp. 659–740). Cambridge, UK: Cambridge

- 513 University Press. doi: 10.1017/CBO9781107415324.018
- 514 Neu, J. L., Flury, T., Manney, G. L., Santee, M. L., Livesey, N. J., & Worden, J.
- 515 (2014, May). Tropospheric ozone variations governed by changes in strato-
- 516 spheric circulation. *Nature Geoscience*, 7(5), 340–344. doi: 10.1038/ngeo2138
- 517 Newell, R. E., Thouret, V., Cho, J. Y. N., Stoller, P., Marenco, A., & Smit, H. G.
- 518 (1999, Mar). Ubiquity of quasi-horizontal layers in the troposphere. *Nature*,
- 519 398(67256725), 316–319. doi: 10.1038/18642
- 520 Newell, R. E., Wu, Z.-X., Zhu, Y., Hu, W., Browell, E. V., Gregory, G. L., ... Liu,
- 521 S. C. (1996). Vertical fine-scale atmospheric structure measured from nasa dc-
- 522 8 during pem-west a. *Journal of Geophysical Research: Atmospheres*, 101(D1),
- 523 1943–1960. doi: 10.1029/95JD02613
- 524 Park, S., Son, S.-W., Jung, M.-I., Park, J., & Park, S. S. (2020, Aug). Evaluation
- 525 of tropospheric ozone reanalyses with independent ozonesonde observations in
- 526 east asia. *Geoscience Letters*, 7(1), 12. doi: 10.1186/s40562-020-00161-9
- 527 Shapiro, M. A. (1980, May). Turbulent mixing within tropopause folds as a mech-
- 528 anism for the exchange of chemical constituents between the stratosphere and
- 529 troposphere. *Journal of the Atmospheric Sciences*, 37(5), 994–1004. doi:
- 530 10.1175/1520-0469(1980)037<0994:TMWTFA>2.0.CO;2
- 531 Skerlak, B., Pfahl, S., Sprenger, M., & Wernli, H. (2019, May). A numerical pro-
- 532 cess study on the rapid transport of stratospheric air down to the surface over
- 533 western north america and the tibetan plateau. *Atmospheric Chemistry and*
- 534 *Physics*, 19(9), 6535–6549. doi: 10.5194/acp-19-6535-2019
- 535 Skerlak, B., Sprenger, M., Pfahl, S., Tyrlis, E., & Wernli, H. (2015). Tropopause
- 536 folds in era-interim: Global climatology and relation to extreme weather
- 537 events. *Journal of Geophysical Research: Atmospheres*, 120(10), 4860–4877.
- 538 doi: <https://doi.org/10.1002/2014JD022787>
- 539 Skerlak, B., Sprenger, M., & Wernli, H. (2014, Jan). A global climatology of
- 540 stratosphere–troposphere exchange using the era-interim data set from
- 541 1979 to 2011. *Atmospheric Chemistry and Physics*, 14(2), 913–937. doi:
- 542 <https://doi.org/10.5194/acp-14-913-2014>
- 543 Spreitzer, E., Attinger, R., Boettcher, M., Forbes, R., Wernli, H., & Joos, H. (2019).
- 544 Modification of potential vorticity near the tropopause by nonconservative
- 545 processes in the ECMWF model. *Journal of the atmospheric sciences*, 76(6),

- 1709–1726.
- Sprenger, M., Maspoli, M. C., & Wernli, H. (2003). Tropopause folds and cross-tropopause exchange: A global investigation based upon ecmwf analyses for the time period march 2000 to february 2001. *Journal of Geophysical Research: Atmospheres*, 108(D12). Retrieved from <https://agupubs.onlinelibrary.wiley.com/doi/abs/10.1029/2002JD002587> doi: <https://doi.org/10.1029/2002JD002587>
- Stohl, A., Bonasoni, P., Cristofanelli, P., Collins, W., Feichter, J., Frank, A., ... Zerefos, C. (2003). Stratosphere-troposphere exchange: A review, and what we have learned from staccato. *Journal of Geophysical Research: Atmospheres*, 108(D12). Retrieved from <https://agupubs.onlinelibrary.wiley.com/doi/abs/10.1029/2002JD002490> doi: <https://doi.org/10.1029/2002JD002490>
- Stoller, P., Cho, J. Y. N., Newell, R. E., Thouret, V., Zhu, Y., Carroll, M. A., ... Sandholm, S. (1999). Measurements of atmospheric layers from the nasa dc-8 and p-3b aircraft during pem-tropics a. *Journal of Geophysical Research: Atmospheres*, 104(D5), 5745–5764. doi: 10.1029/98JD02717
- Thouret, V., Cho, J. Y. N., Newell, R. E., Marenco, A., & Smit, H. G. J. (2000). General characteristics of tropospheric trace constituent layers observed in the mozaic program. *Journal of Geophysical Research: Atmospheres*, 105(D13), 17379–17392. doi: 10.1029/2000JD900238
- Trickl, T., Bärtsch-Ritter, N., Eisele, H., Furger, M., Mücke, R., Sprenger, M., & Stohl, A. (2011, Sep). High-ozone layers in the middle and upper troposphere above central europe: potential import from the stratosphere along the subtropical jet stream. *Atmospheric Chemistry and Physics*, 11(17), 9343–9366. doi: 10.5194/acp-11-9343-2011
- Trickl, T., Feldmann, H., Kanter, H.-J., Scheel, H.-E., Sprenger, M., Stohl, A., & Wernli, H. (2010, Jan). Forecasted deep stratospheric intrusions over central europe: case studies and climatologies. *Atmospheric Chemistry and Physics*, 10(2), 499–524. doi: 10.5194/acp-10-499-2010
- Trickl, T., Vogelmann, H., Ries, L., & Sprenger, M. (2020, Jan). Very high stratospheric influence observed in the free troposphere over the northern alps – just a local phenomenon? *Atmospheric Chemistry and Physics*, 20(1), 243–266.

- doi: 10.5194/acp-20-243-2020
- Tyrlis, E., Skerlak, B., Sprenger, M., Wernli, H., Zittis, G., & Lelieveld, J. (2014). On the linkage between the asian summer monsoon and tropopause fold activity over the eastern mediterranean and the middle east. *Journal of Geophysical Research: Atmospheres*, 119(6), 3202–3221. doi: <https://doi.org/10.1002/2013JD021113>
- Wagner, A., Bennouna, Y., Blechschmidt, A.-M., Brasseur, G., Chabrillat, S., Christophe, Y., ... Zerefos, C. (2021, May). Comprehensive evaluation of the copernicus atmosphere monitoring service (cams) reanalysis against independent observations: Reactive gases. *Elementa: Science of the Anthropocene*, 9(1), 00171. doi: 10.1525/elementa.2020.00171
- Wang, X., Wu, Y., Randel, W., & Tilmes, S. (2020, Oct). Stratospheric contribution to the summertime high surface ozone events over the western united states. *Environmental Research Letters*, 15(10), 1040a6. doi: 10.1088/1748-9326/abba53
- Wargan, K., Labow, G., Frith, S., Pawson, S., Livesey, N., & Partyka, G. (2017, Apr). Evaluation of the ozone fields in nasa’s merra-2 reanalysis. *Journal of Climate*, 30(8), 2961–2988. doi: 10.1175/JCLI-D-16-0699.1
- Williams, R. S., Hegglin, M. I., Kerridge, B. J., Jöckel, P., Latter, B. G., & Plummer, D. A. (2019, Mar). Characterising the seasonal and geographical variability in tropospheric ozone, stratospheric influence and recent changes. *Atmospheric Chemistry and Physics*, 19(6), 3589–3620. doi: 10.5194/acp-19-3589-2019
- Zanis, P., Hadjinicolaou, P., Pozzer, A., Tyrlis, E., Dafka, S., Mihalopoulos, N., & Lelieveld, J. (2014, Jan). Summertime free-tropospheric ozone pool over the eastern mediterranean/middle east. *Atmospheric Chemistry and Physics*, 14(1), 115–132. doi: 10.5194/acp-14-115-2014
- Zhuang, J., Jacob, D. J., & Eastham, S. D. (2018, May). The importance of vertical resolution in the free troposphere for modeling intercontinental plumes. *Atmospheric Chemistry and Physics*, 18(8), 6039–6055. doi: 10.5194/acp-18-6039-2018